# High Impedance Faults Detection Technique Based on Wavelet Transform

MING-TA YANG[1], JIN-LUNG GUAN[2], JHY-CHERNG GU[3]
Department of Electrical Engineering
St. John's University, #499, Sec. 4, Tamking Rd., Tamsui, Taipei Hsien, Taiwan[1]
Hwa Hsia Institute of Technology, #111 Gong Jhuan Rd., Chung Ho, Taipei Hsien, Taiwan[2]
National Taiwan University of Science and Technology, #43, Sec. 4, Keelung Rd., Taipei, Taiwan[3]
Taiwan

http://www.sju.edu.tw[1] http://www.hwh.edu.tw[2] http://www.ntust.edu.tw[3]

*Abstract:* -The purpose of this paper is to solve the problem of protecting aerial lines from high impedance faults (HIFs) in distribution systems. This investigation successfully applies $3I_0$ zero sequence current to solve HIF problems. The feature extraction system based on discrete wavelet transform (DWT) and the feature identification technique found on statistical confidence are then applied to discriminate effectively between the HIFs and the switch operations. Based on continuous wavelet transform (CWT) pattern recognition of HIFs is proposed, also. Staged fault testing results demonstrate that the proposed wavelet based algorithm is feasible performance well.

*Key-Words:* -continuous wavelet transform, discrete wavelet transform, high impedance faults, statistical confidence

## 1 Introduction

Protection of aerial lines from HIFs is serious business for electric utilities. HIFs can be described as an abnormal event on distribution system which does not detected by traditional protection devices with sufficient fault current.

The existing detection techniques may be categorized into three classes, time domain, frequency domain and wavelet transform. The time domain detection algorithms include electromechanical relay and artificial neural network based relaying. A ratio-ground-relaying has been proposed by researchers at Westinghouse Electric Corporation and Pennsylvania power & Light [1]. A smart relaying algorithm based on graphical image feature extraction using time domain transient signals. The algorithm uses the random behavior of the arcing fault current [2]. The detection algorithm of the frequency domain applies Fourier transform to extract the features of the harmonic components. The identification approach involved third harmonic current [3], statistical pattern recognition approach [4], energy technique [5], randomness technique [6], half cycle asymmetry [7] and amplitude ratio technique [8]. Wavelet transform can be employed to examine the transient phenomena of HIFs signals in both the time and frequency domains. The algorithm is ideally for nonstationary signals such as those encountered under HIF arcing faults [9-10].

## 2 Wavelet Based HIFs Detection

The wavelet based algorithm HIFs detection system includes two individual algorithms for individually detecting HIFs are shown in Fig. 1. These relaying algorithms are based on CWT and DWT.

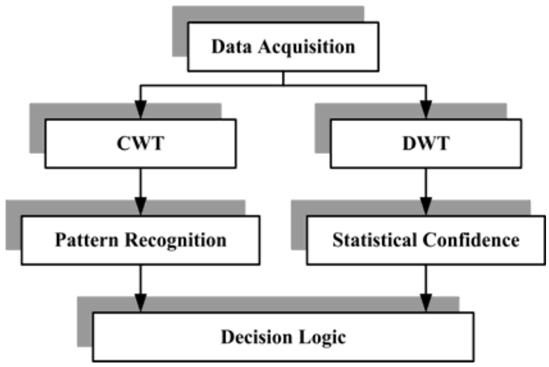


Fig. 1. Wavelet based algorithm HIFs detection system

### 2.1 Wavelet Transform

The simple time domain representation of the signal itself gives the localization in time. A wavelet representation will give the location in both time and frequency simultaneously. The literatures demonstrate that the sharp signal variations can be regarded as features of the faults.

This investigation utilized the wavelet transform (WT) as a feature extraction tool. Wavelet transform can be employed to examine the transient phenomena of HIFs signals in both the time and frequency domains. The proposed approach is to detect the HIFs using the multiresolution analysis (MRA) output. The MRA can easily extract important features implicit in the distribution feeder voltage and current signals, even when these features are very weak [11]. Filter bank theory provides efficient computational schemes for wavelet analysis. Selecting an adequate wavelet filter is vital to identifying the HIF features of 3I0 zero sequence current. The "optimal" wavelet for extracting a given signal is that which can generate the most coefficients with maximal values within the time-scale domain, to represent the feature of a signal. This wavelet should also have sharp cut-off frequencies. This study employed the Daubechies D-20 (denoted Db10) wavelet, since it has been demonstrated to perform well and satisfy the aforementioned conditions. In this study, the sampling frequency $f_s$ was set to 6 kHz, and the resolution level of the MRA filter banks was set to 5.

## 2.2 Statistical Confidence [12]

A self-turning scheme based on the chi-square distribution and 95% confidence interval (CI) is applied to set the threshold level automatically for the DWT coefficients of $3I_0$ zero sequence current variances examined.

The HIF identification criterion in this study is based on features extracted from the DWT detail and approximation coefficients. The magnitude of the DWT details and approximations are a normal distribution random variable. Let $X_1, X_2, \ldots, X_n$ be a random sample from a DWT coefficient with mean $\mu$ and variance $\sigma^2$, and let $S^2$ denote the sample variance.

Then, the random variable $X^2 = \frac{(n-1)S^2}{\sigma^2}$ has a chi-square $(\chi^2)$ distribution with n-1 degrees of freedom.

If $X \sim N(\mu, \sigma^2)$ and $Z = \frac{(X-\mu)^2}{\sigma^2}$, then

$$Z = \frac{(X-\mu)^2}{\sigma^2} \sim \chi_1^2 \quad (1)$$

The random variable $Z$ has a chi-square $(\chi^2)$ distribution with 1 degree of freedom. The 95% CI on $\sigma^2$ is constructed as

$$P\left[Z \le \chi^2_{1,0.05}\right] = 1-0.05 = 0.95 \quad (2)$$

From Equ. (2) and the confidence internal for $\sigma$, the threshold can be derived as

$$X_{threshold} = \mu + \sqrt{\chi^2_{1,0.05} \times \sigma^2} \quad (3)$$

To enhance the reliability of HIFs detection the confidence level was adopted to identify the abnormal variation.

The analysis of the staged test data reveals that intermittent arcing phenomena arose in most HIFs, and that the waveform of the arcing current had an unsymmetrical shape in each cycle. The same was true of arcing in switching transient condition of load or capacitor bank, except for the sustained time of arcing, which was longer in the HIFs than in the switching transient. Hence, the statistical confidence was applied for DWT details and approximations estimation. Detection system will indicate an HIF if statistical confidence of DWT coefficients is above threshold, or excessive differences between successive samples.

# 3 Staged Fault Testing for HIFs

An 11.4 kV Tai-16 feeder served from Taishi substation Yunlin Administration Division of Taipower near Mailiao, was chosen as the testing site [13]. This feeder mostly supplies aquaculture load, and has an average load of about 100－110A.

The HIF faults were staged at electric pole #61, and tested on either the ground or ground objects, which were dry and wet sand, gravel, asphalt, concrete, grass, tussock, shrub and electric pole. Additionally, a broken conductor was tested in air for HIFs. An XLPE covered conductor, a copper bare conductor and ACSR were employed in these tests. The 59 faults were staged on phase A, B, and C, and three capacitor banks switching tests executed.

# 4 Test Results

Fig. 2, 5, 8 and 11 respectively shows the five-level wavelet analysis of $3I_0$ zero sequence current for an XLPE conductor HIF occurred at roughly 0.6s and after 6.3s on shrub, 4s on gravel, 5.8s on tussock and a copper bare conductor HIF occurred at around 0.5s on wet asphalt. The result of calculation of 95% confidence internal threshold of wavelet coefficients of $3I_0$ zero sequence rms current is shown in Fig. 3, 6, 9, 12 respectively.

Observation of Fig. 3, 6, 9 and 12 suggests the following comments. Wavelet coefficients $c_5[n]$, $d_5[n]$, $d_4[n]$, $d_3[n]$ and $d_2[n]$ will be selected to identify HIFs. Once statistical confidence of DWT coefficients is higher than setting threshold or excessive differences between successive samples, detection system will issue HIF event. According to the foregoing criteria, the DWT based detection system recognizes HIF at 1s and 7s, 5s, 7s, 1s respectively.

For relevant entities of HIFs, the CWT method allows to obtain result better or similar to those carried out by the DWT. The Fig. 4, 7, 10, 13 respectively shows 3D CWT of $3I_0$ zero sequence current.

Fig. 14 demonstrates the five-level wavelet analysis of $3I_0$ zero sequence current for capacitor banks switching occurred at approximately 4.3s. The result of calculation of 95% CI threshold of a capacitor bank switching is different from the HIF events as shown in Fig. 15. In Fig. 16 shows 3D CWT.

The overall success rate of detection system in discriminating classes was around 93.2% (55/59). An HIF was incorrectly identified 4 times. Since the sustained time of the capacitor banks switching was not longer than the HIF arcing, three capacitor banks switching events were detected properly.

## 5 Conclusions

This paper is intended as an investigation of staged HIFs testing signals using DWT and CWT, in order to extract signal features that can be used for identification. The WT is based on a dyadic decomposition structure. WT expands a signal not in terms of trigonometric polynomial but by wavelets, generated via the scaling and the translation of a fixed wavelet function. The wavelet function is localized in time and frequency domains yielding wavelet coefficients at different scales. Correspondingly, the WT provide more detailed information by applying a shorter window to the higher frequency contents of the signal. Therefore, the WT is suggested as a suitable solution for analyzing fault signals during HIF. The statistical confidence of DWT coefficients is adopted as the criteria of HIF identification. This approach not only retains the characteristic of the original coefficients, but also accelerates the HIF recognition. The test results showed that the proposed detection system identifies HIF more accurately than other available relaying algorithms.

*References:*

[1]H. Calhoun, M. T. Bishop, C. H. Eichler, and R. E. Lee, Development and testing of an electro-mechanical relay to detect fallen distribution conductors, *IEEE Trans. Power Apparatus and Systems,* June 1982, Vol. PAS-101, No. 6, pp. 1643-1650.

[2]A. M. Sharaf and S. I. Abu-Azab, A smart relaying scheme for high impedance faults in distribution and utilization networks, in *Proc. of the Canadian Conf. on Electrical and Computer Engineering*, March 2000, Vol. 2, 7-10, pp. 740-744.

[3]Hughes Aircraft Company, High Impedance Fault Detection using Third Harmonic Current, *EPRI Research Project 1285-2, Final Report EL-2430*, June 1982.

[4]Detection of High Impedance Faults, *EPRI Report EL-2413*, prepared by Power Technologies, Inc. June 1982.

[5]B. M. Aucoin and B. D. Russell, Distribution high impedance fault detection using high frequency current components, *IEEE Trans. Power Apparatus system,* June 1982, Vol. PAS-101, No. 6, pp1596-1606.

[6]B. D. Russell and R. P. Chinchali, A digital signal processing algorithm for detecting arcing faults on power distribution feeders, *IEEE Trans. Power Delivery*, January 1989, Vol. 4, No. 1, pp. 132-140.

[7]W. H. Kwon et al, High Impedance Fault Detection Utilizing Incremental Variance of Normalized Even Order Harmonic Power, in *Proc. IEEE/PES 1990 Summer Meeting*, July 15-19, 1990, Paper No. 90 SM 349-1.

[8]A. F. Sultan, G. W. Swift and D. J. Fedirchuk, Detecting Arcing Downed-Wires Using Fault Current Flicker and Half-Cycle Asymmetry, *IEEE Trans. on Power Delivery*, 1994, Vol. 9 No. 1, pp. 461-470.

[9]A. Lazkano, J. Ruiz, E. Aramendi, and L. A. Leturiondo, A new approach to high impedance fault detection using wavelet packet analysis, in *Proc. IEEE 2000 Int. Conf. on Harmonics and Quality of Power*, 2000, pp. 1005-1010.

[10]D. C. T. Wai and X. Yibin, A novel technique for high impedance fault identification, *IEEE Trans. Power Delivery*, July 1998, Vol. 13, No. 3, pp. 738-744.

[11]O. A. S. Youssef, A wavelet-based technique for discrimination between faults and magnetizing inrush currents in transformers, *IEEE Trans. Power Delivery*, Nov. 2003, Vol. 18, No. 1, pp. 170-176.

[12]D. C. Montgomery and G. C. Runger, *Applied Statistics and Probability for Engineers*, New York: John Wiley & Sons, 2003, ch. 8.

[13]Ming-Ta Yang, Jhy-Cherng Gu, Jin-Lung Guan and Chau-Yuan Cheng, Evaluation of algorithms for high impedance faults identification based on staged fault tests, in *Proc. IEEE/PES 2006 General Meeting*, June 18-22, 2006, pp. 1-8.

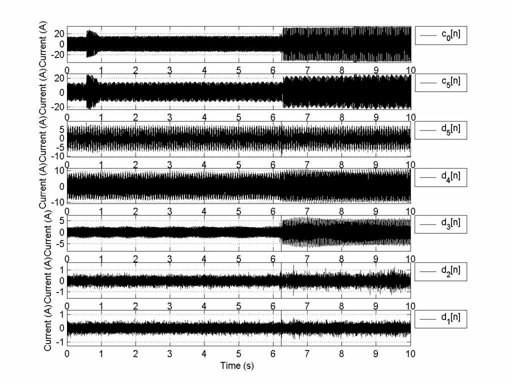


(a)

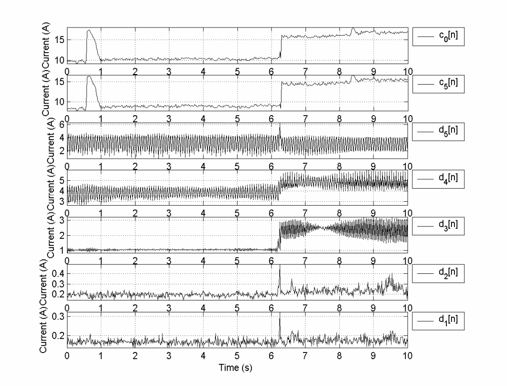


(b)

Fig. 2. XLPE conductor phase A HIF on shrub: five-level wavelet analysis of $3I_0$ zero sequence (a): instantaneous current (b): rms current

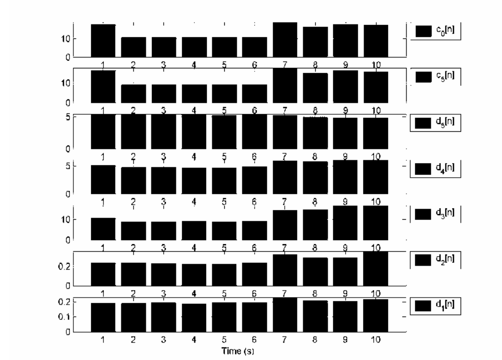


Fig. 3. XLPE conductor phase A HIF on shrub: 95% CI threshold of wavelet coefficients of $3I_0$

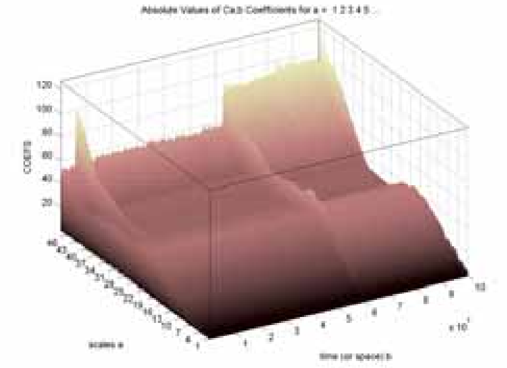


Fig. 4. XLPE conductor phase A HIF on shrub: CWT of $3I_0$

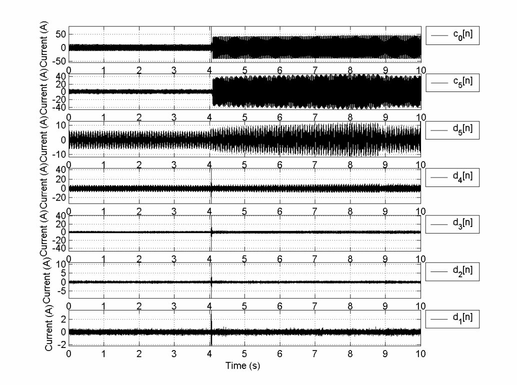


(a)

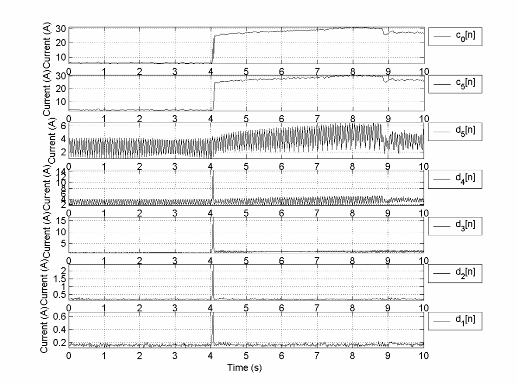


(b)

Fig. 5. XLPE conductor phase A HIF on gravel: five-level wavelet analysis of $3I_0$ zero sequence (a): instantaneous current (b): rms current

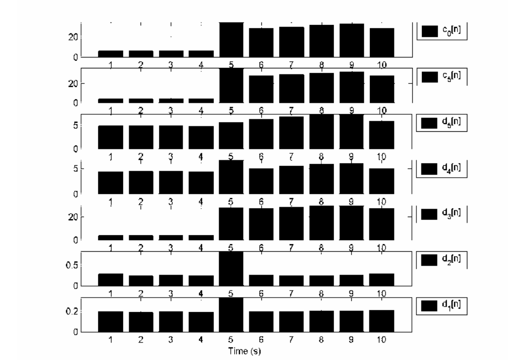


Fig. 6. XLPE conductor phase A HIF on gravel: 95% CI threshold of wavelet coefficients of $3I_0$

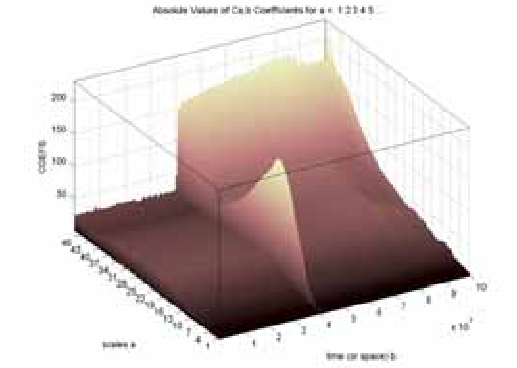


Fig. 7. XLPE conductor phase A HIF on gravel: CWT of $3I_0$

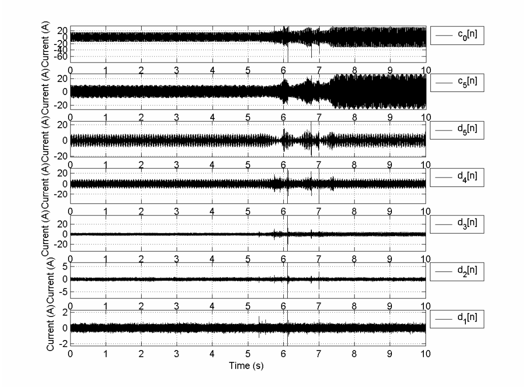


(a)

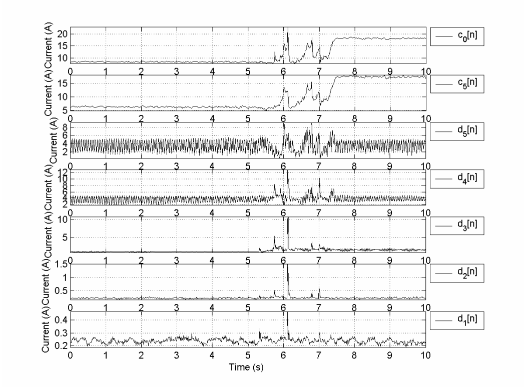


(b)

Fig. 8. XLPE conductor phase A HIF on tussock: five-level wavelet analysis of $3I_0$ zero sequence (a): instantaneous current (b): rms current

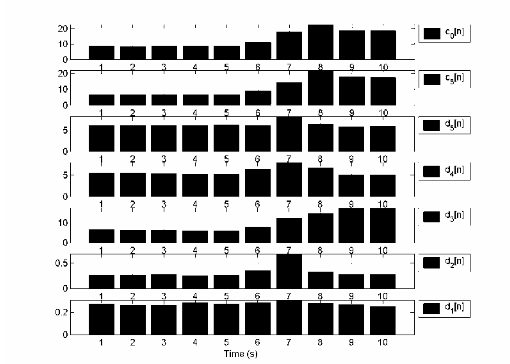


Fig. 9. XLPE conductor phase A HIF on tussock: 95% CI threshold of wavelet coefficients of $3I_0$

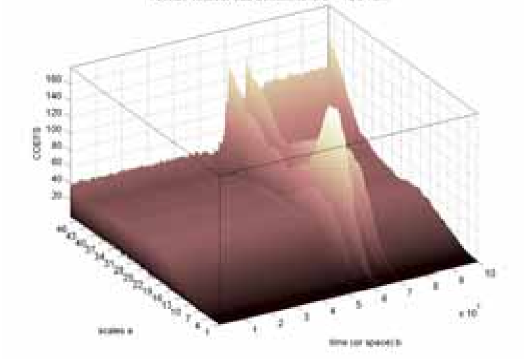

Fig. 10. XLPE conductor phase A HIF on tussock: CWT of $3I_0$

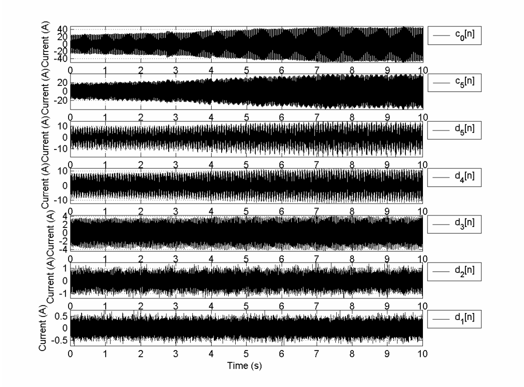


(a)

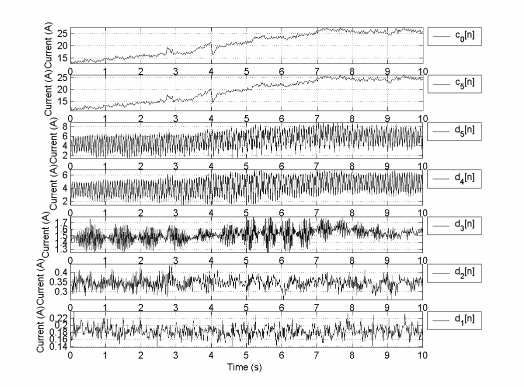


(b)

Fig. 11. Copper bare conductor phase A HIF on wet asphalt: five-level wavelet analysis of $3I_0$ zero sequence (a): instantaneous current (b): rms current

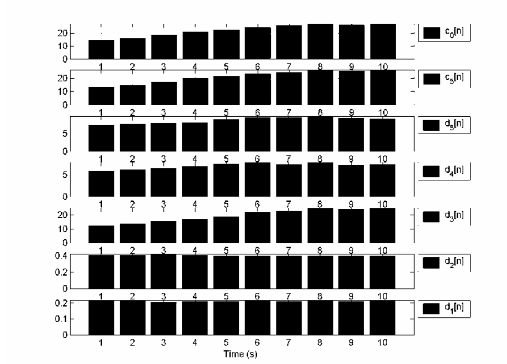


Fig. 12. XLPE conductor phase A HIF on wet asphalt: 95% CI threshold of wavelet coefficients of $3I_0$

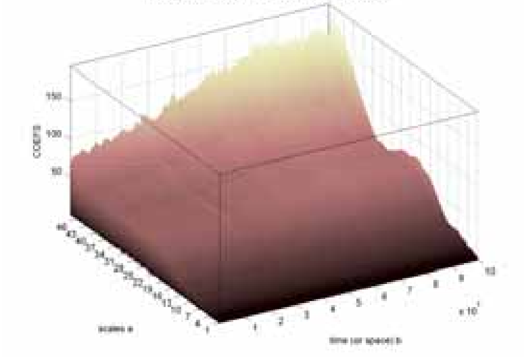

Fig. 13. XLPE conductor phase A HIF on wet asphalt: CWT of $3I_0$

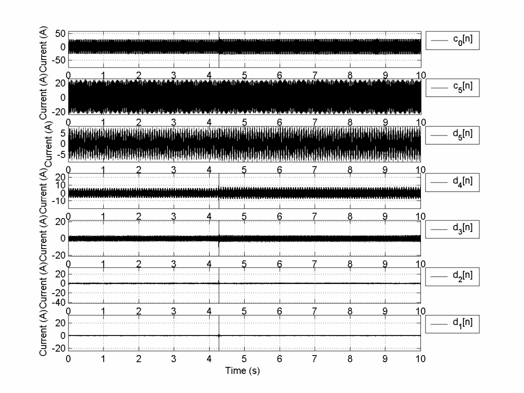


(a)

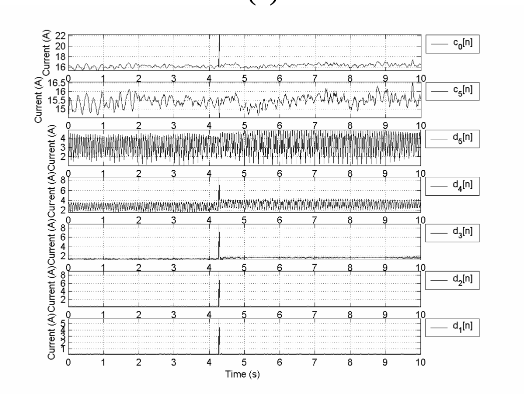


(b)

Fig. 14. Capacitor bank switching: five-level wavelet analysis of $3I_0$ zero sequence (a): instantaneous current (b): rms current

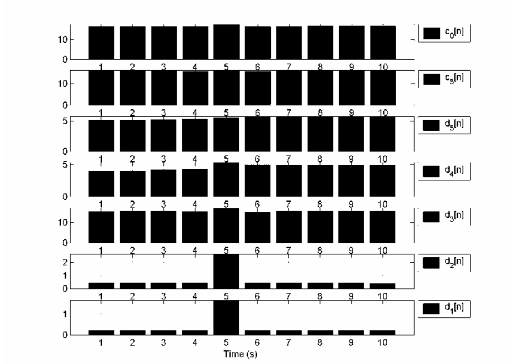


Fig. 15. Capacitor bank switching: 95% CI threshold of wavelet coefficients of $3I_0$

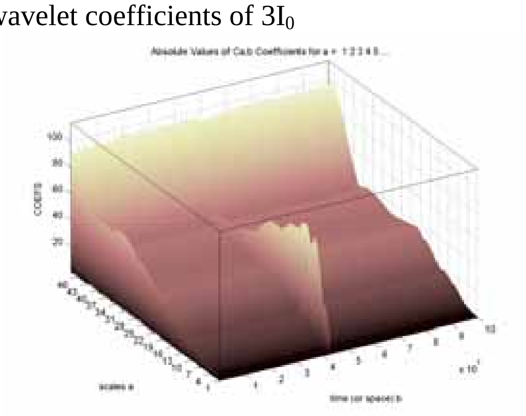

Fig. 16. Capacitor bank switching: CWT of $3I_0$